60335 BASALTIC IMPACT MELT 318 g

INTRODUCTION: 60335 is a tough, medium gray, basaltic impact melt with a pronounced vug population (Fig. 1). The rock as a whole is homogeneous although the grain size changes abruptly and color varies irregularly from dark to light areas. Metal spherules (up to 5 mm) are abundant.

60335 was collected about 70 m east-northeast of the Lunar Module, where it was 1/3 to 1/2 buried with a moderately well-developed fillet. Its orientation is known; zap pits are present on all surfaces but one, although the densities vary considerably from surface to surface.

FIGURE 1. S-72-38289.

PETROLOGY: Walker et al. (1973), Brown et al. (1973), Nord et al. (1973) and Vaniman and Papike (1981) provide petrographic information. Nord et al.(1973) studied pyroxene exsolution using high-voltage transmission electron microscopy. Misra and Taylor (1975) report metal and schreibersite compositions.

60335 is a basaltic impact melt rock that exhibits a variety of melt textures (Fig. 2). Most commonly, normally zoned, subhedral plagioclase phenocrysts (An_{95-86}) and shocked, anhedral plagioclase xenocrysts (An_{97-95}, up to 4 mm) grade into a finer grained matrix of equant to lathy plagioclase partially enclosed by olivine (Fo_{85-79}, single crystals up to 10 mm). In other areas a Si-K-rich glassy mesostasis fills the interstices. Overgrowths of orthopyroxene (Wo_5En_{76}), pigeonite (Wo_9En_{76}) and augite occasionally rim the olivines

and many of the plagioclase phenocrysts display a clear rim over a shocked core. Pigeonite occasionally shows augite exsolution lamellae. A mode of the matrix given by Walker et al. (1973) is reproduced as Table 1. Minor phases include silica, phosphates, Zr-armalcolite, ilmenite, ulvospinel, metal and schreibersite. Mineral compositions are given in Figures 3 and 4.

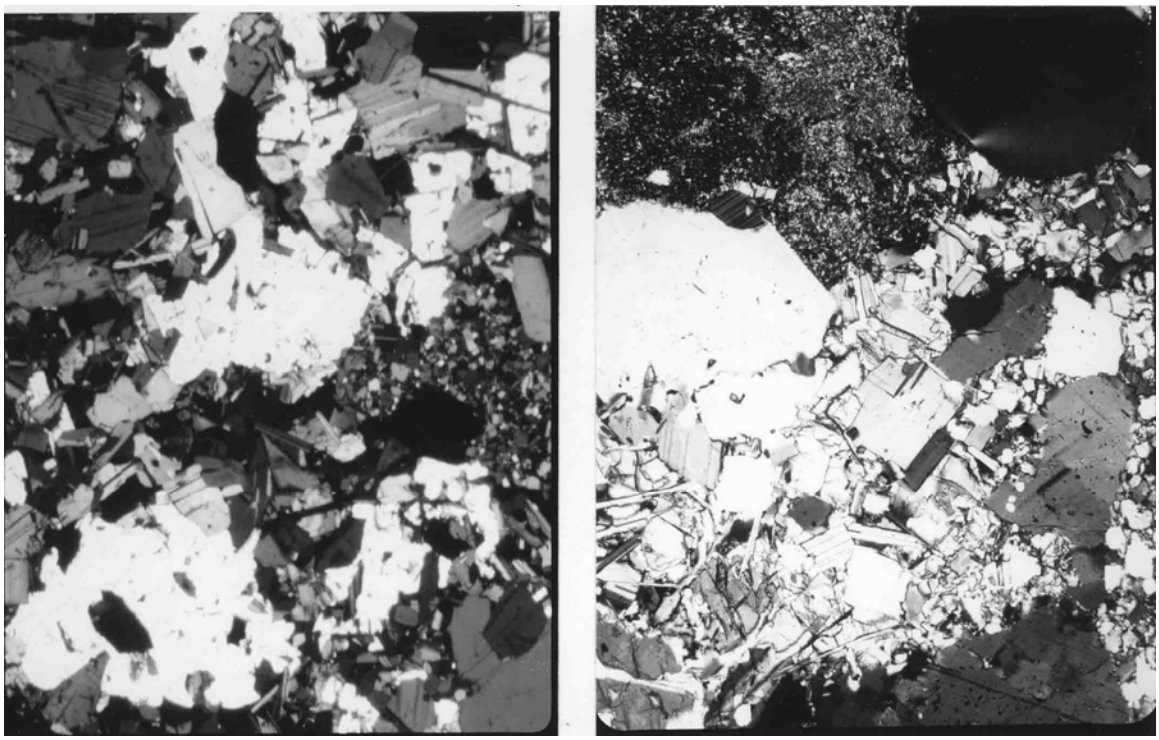

FIGURE 2.
a) 60335,61. General basaltic, xpl. Width 2 mm.
b) poikilitic area (top left) and vesicle (top right) in general basaltic area, xpl. Width 1 mm.

Less common melt textures in this rock include radiating clusters of plagioclase, often cored by an incompletely digested clast and poikilitic patches in which 0.5 mm olivine encloses many small clasts and crystallites of plagioclase (Fig.2). Although Walker et al. (1973) and the Apollo 16 Lunar Sample Information Catalog (1972) interpret certain poikilitic areas as lithic clasts, an extensive survey of library thin sections convinces us that these patches crystallized from the same melt that produced the bulk of the rock. Evidence for this interpretation includes the arcuate boundaries of the patches against vesicles (Fig. 2), the tendency of the poikilitic patches to completely fill irregularly shaped areas and the fact that some of the poikilitic olivines are single crystals with olivines that are definitely a part of the ophitic matrix.

Lithic clasts include granoblastic anorthosite (2 mm) and granoblastic troctolite (5 mm) with accessory ilmenite and metal. Most of the lithic clasts are shocked with a well defined reaction rim of fine-grained, unshocked plagioclase.

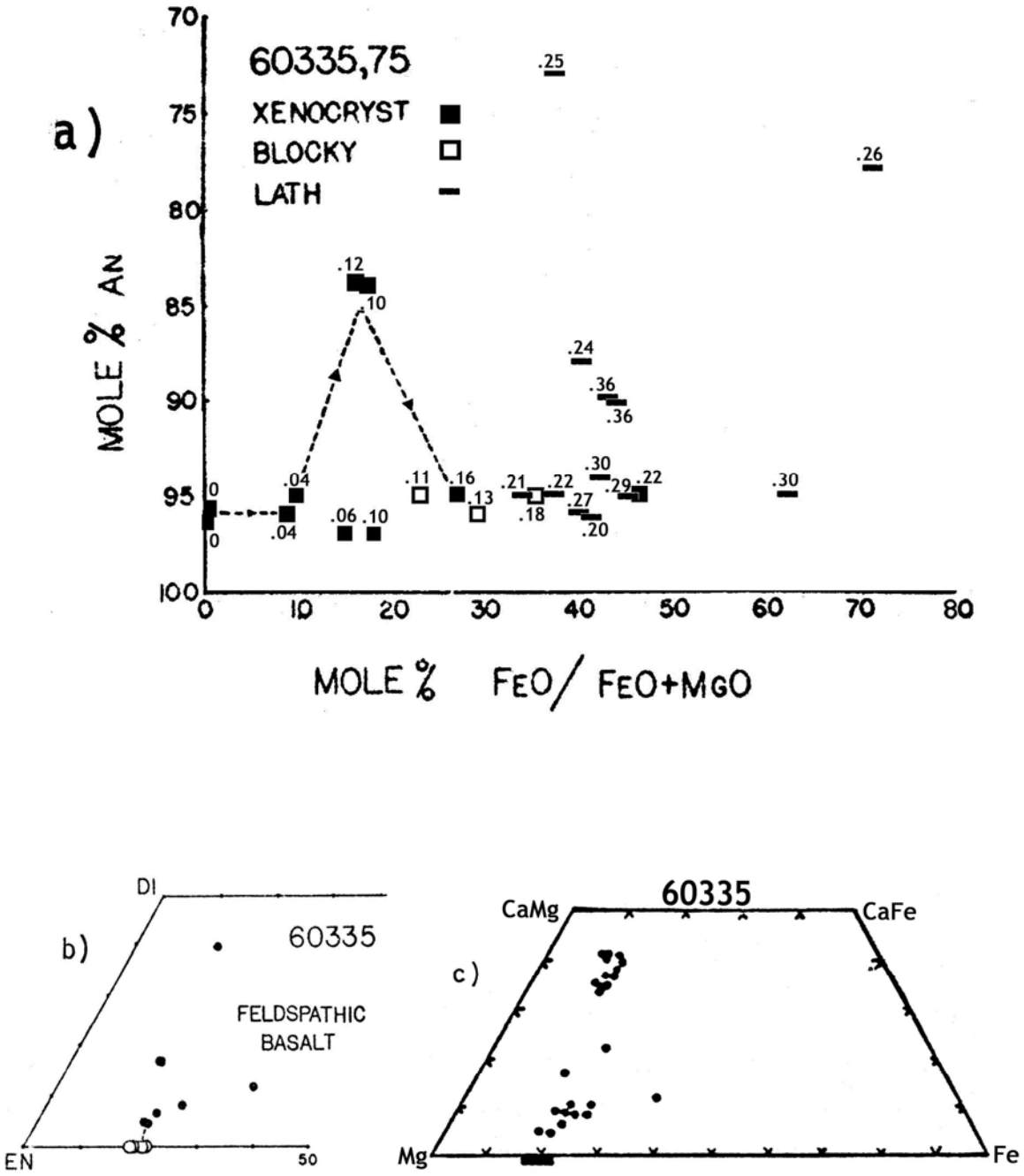

FIGURE 3. Mineral compositions;
a) plagioclases, from Walker et al.(1973).
b) pyroxenes, from Walker et al.(1973).
c) pyroxenes, from Vaniman and Papike (1981).

EXPERIMENTAL PETROLOGY: Muan et al. (1974) and Ford et al. (1974) report experimentally determined equilibrium phase relations. At low pressure plagioclase is the liquidus phase of 60335, followed by spinel, then olivine. Liquidus temperature is >1370°C. Spinel becomes unstable between 1200-1216°C. At 1 kb pressure with 10% water, spinel is the liquidus phase at temperatures >1250°C (Ford et al., 1974).

TABLE 1. Mode of 60335 from Walker et al. (1973).

Plagioclase	64%
Olivine	16%
Clinopyroxene	10%
Opaques	2%
Glassy mesostasis	8%
Orthopyroxene	tr

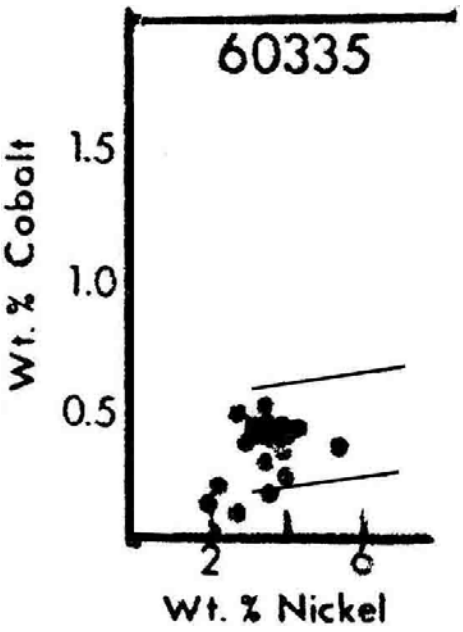

FIGURE 4. Metals; from Misra and Taylor (l975).

L.A. Taylor et al.(1976) performed subsolidus heating experiments to observe changes in metal grain morphology and chemistry. The most conspicuous textural change observed was the development of euhedral metal crystals at the edges of the annealed fragments. Observed changes in metal compositions are summarized in Figure 5.

CHEMISTRY: Major and trace element data are given by Haskin et al. (1973), Rose et al. (1973), Miller et al. (1974), Fruchter et al.(1974) (of ,34 erroneously reported as ,4) Wanke et al. (1976) and LSPET (1973). Hubbard et al.(1974) and Ehmann and Chyi (1974) report trace elements, Clark and Keith (1973) provide data on natural and cosmogenic radionuclides and Barnes et al. (1973) present trace element and isotopic abundances (see also STABLE ISOTOPES and GEOCHRONOLOGY below). Walker et al. (1973) report major elements determined by electron microprobe analyses of natural rock powder fused to a glass.

Chemically 60335 is a very homogeneous rock. Its major element composition is that of anorthositic norite (Table 2 and Fig. 6), very similar to the local mature soils. Rare earth elements (Fig. 7) are slightly higher in the rock (La ~ 65x chondrites) than in the local soils (La ~45x chondrites). The Zr/Hf is high, dominated by a KREEP component (Ehmann and Chyi, 1974). Siderophiles indicate a substantial meteoritic contribution (Table 2).

Sato (1976) measured the oxygen fugacity of 60335 directly using the solid-electrolyte oxygen cell method. The low values (Table 3) are consistent with the equilibration of metallic iron with the silicate and oxide phases. A slight self-reduction was noted during the first heating cycle.

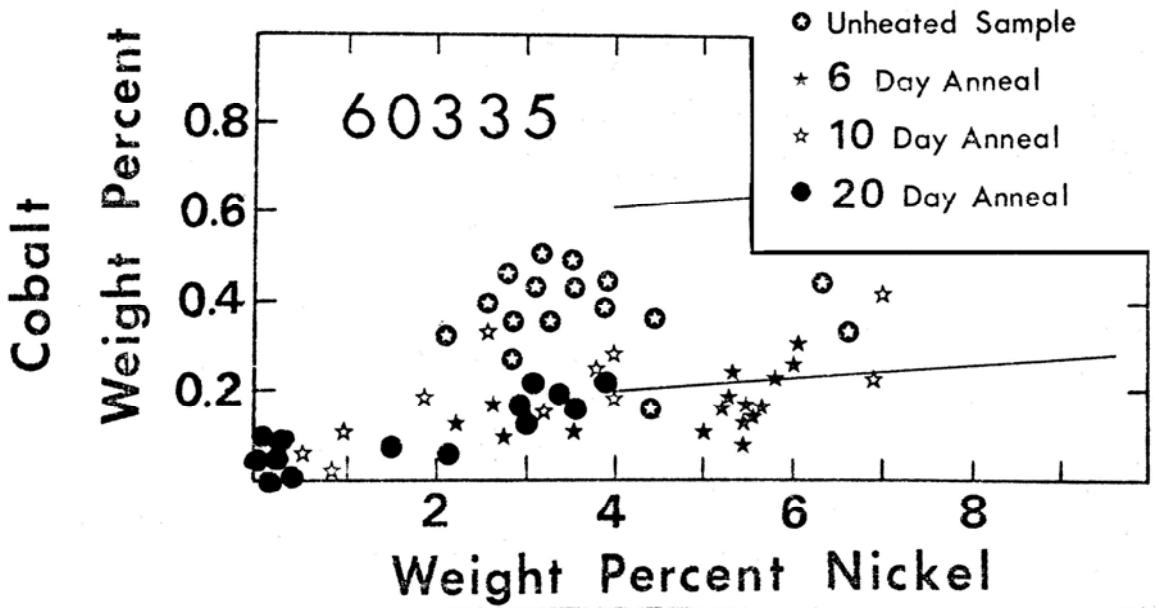

FIGURE 5. Subsolidus metal changes;
from L. Taylor et a1.(1976).

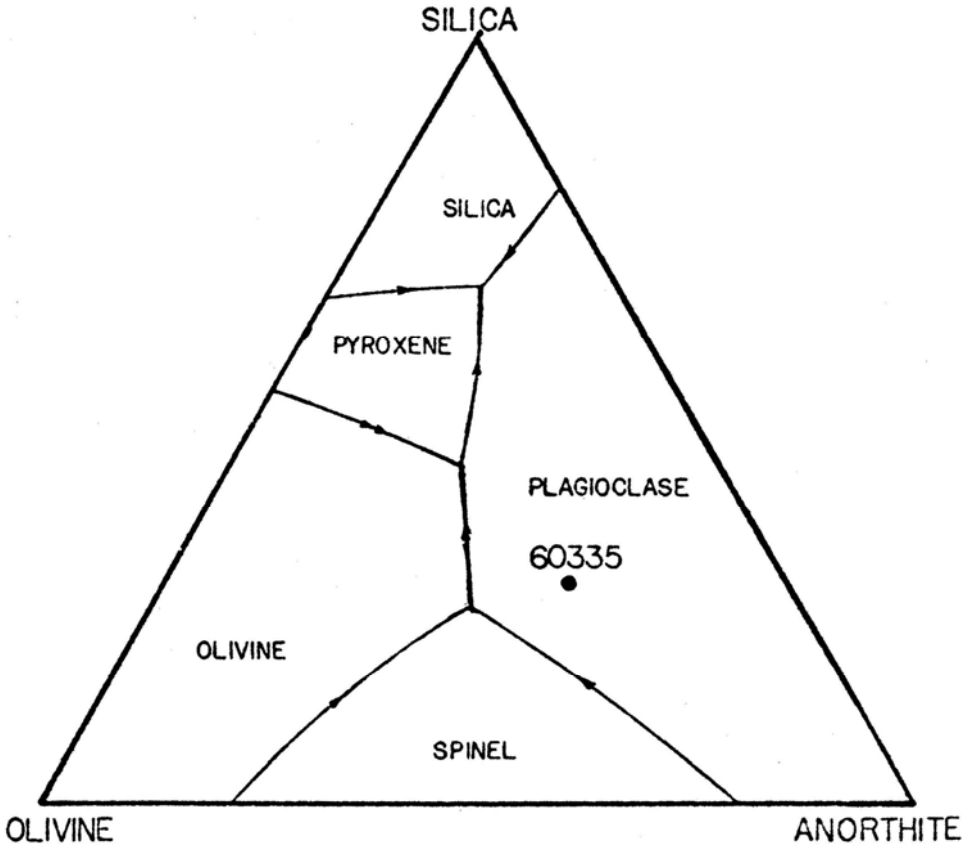

FIGURE 6. From Walker et al. (1973).

STABLE ISOTOPES: Barnes et al, (1973) provide data on isotopes of Cr, Ni and K.

RADIOGENIC ISOTOPES AND GEOCHRONOLOGY: Whole rock Rb-Sr data are provided by Barnes et al. (1973) and Nyquist et al. (1974). A model age of 4.055 b.y. was calculated by Barnes et al. (1973) assuming I = 0.6994 (sic.). Model ages of T_{BABI} = 4.19 ± 0.06 b.y. and T_{LUNI} = 4.23 ± 0.06 b.y. were calculated by Nyquist et al. (1974).

Whole rock U-Th-Pb isotopic data are reported by Barnes et al. (1973). Four model ages ranging from 4.059 - 4.081 b.y. and averaging 4.070 b.y. were calculated. 60335 is concordant at 4.075 b.y.

Relative isotopic compositions of ^{39}K, ^{40}K and ^{41}K are given by Barnes et al.(1973).

RARE GAS/EXPOSURE AGE: Solar flare track data indicate that 60335 had a complex exposure history (Fig. 8) but allow an approximate burial (subdecimeter) age of 50 m.y. and a surface exposure age of ~0.5 m.y. to be calculated (Bhandari et al., 1976). Bhandari (1977) reports a ^{26}Al surface exposure age of < 0.2 m.y. ^{26}Al other cosmic-ray induced radionuclide abundance data are provided by Clark and Keith (1973).

TABLE 2. Summary chemistry of 60335.

SiO_2	46.0
TiO_2	0.61
Al_2O_3	24.9
Cr_2O_3	0.13
FeO	4.7
MnO	0.07
MgO	8.1
CaO	14.3
Na_2O	0.57
K_2O	0.25
P_2O_5	0.21
Sr	150
La	21
Lu	0.84
Rb	6.8
Sc	8.1
Ni	340
Co	20
Ir ppb	17
Au ppb	16.8
C	
N	
S	
Zn	2
Cu	8

Oxides in wt%; others in ppm except as noted.

TABLE 3. Average oxygen fugacity of 60335.

T (°C)	-log fo_2(atm)
1000	16.7
1050	15.6
1100	14.6
1150	13.7
1200	12.8

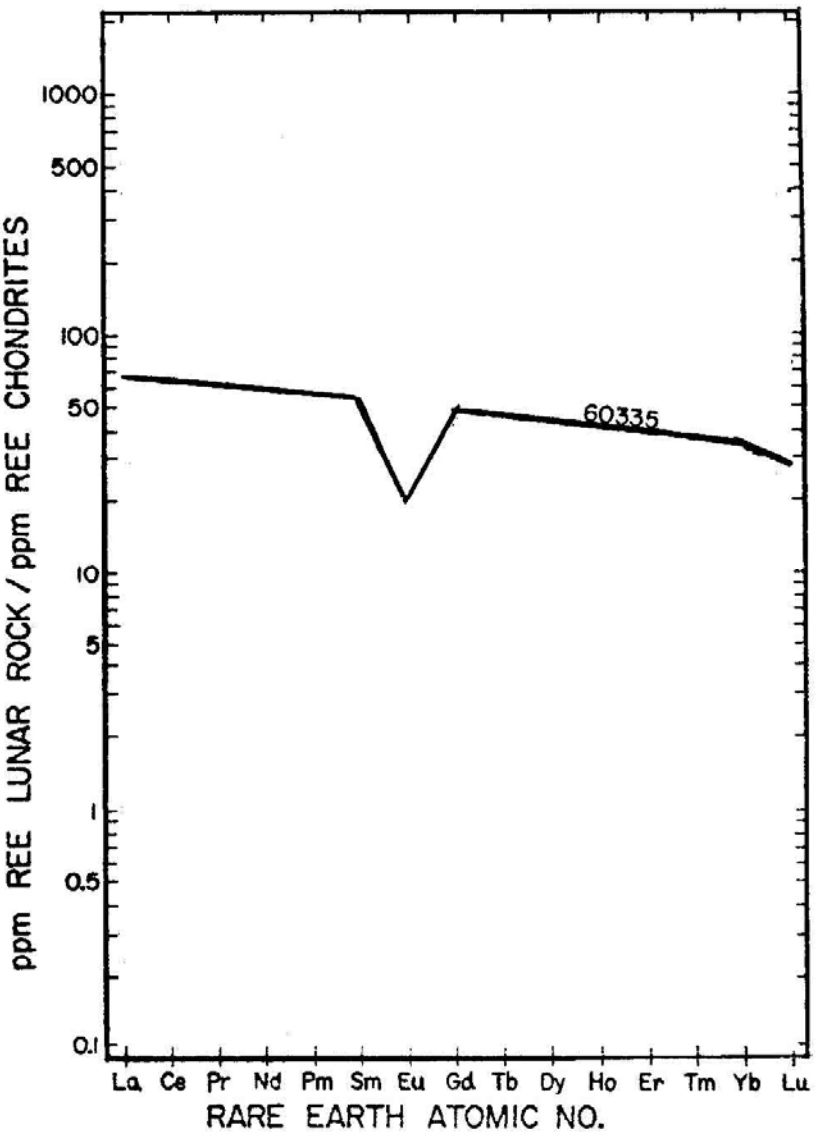

FIGURE 7. Rare earths; from Haskin et al.(1973).

MICROCRATERS AND TRACKS: Morrison et al. (1973) and Neukum et al. (1973) provide size-frequency data on microcraters. Morrison et al. (1973) note the exceptionally low frequency of craters on 60335 and calculate "best estimate" exposure age of 0.6 - 0.8 m.y.

PHYSICAL PROPERTIES: 60335 is the "LPM" rock, chosen to measure the in situ remanent magnetization of a lunar sample using the Lunar Portable Magnetometer. Measurements made with the LPM on the lunar surface and in the laboratory did not detect any rock magnetization (Dyal et al., 1972). Pearce et al. (1973) report the total remanence of 60335 as 5.4×10^{-6} emu/g, confirming that its intensity is well below the resolution of the LPM. Thus the amount of lunar-induced soft remanence in this sample could not be determined.

Intrinsic and remanent magnetic properties were measured on two chips of 60335 by Pearce et al. (1973) using room temperature hysteresis loops and AF-demagnetization techniques. Total metal content is 0.36 wt%, principally as multidomain particles. The Curie temperature ($\theta = 760°C$) is characteristic of iron with a few percent Ni. A low Curie temperature ($\theta' = 350°C$) phase, possibly high-Ni metal, was also detected. Electron microprobe studies did not detect such a high-Ni metal phase (Misra and Taylor, 1975). Chou and Pearce (1976) note that 60335 has Ni/metal slightly higher than the local soils and interpret this as indicating that very little metal in the rock was produced by subsolidus reduction.

AF-demagnetization of the two chips revealed significant differences between the chip that was stored in field-free space (,30) and the chip that was not (,18) (Fig. 9). Apparently the rock acquired a non-lunar viscous remanence that is stable against AF-demagnetization but not against field-free storage (Pearce et al., 1973).

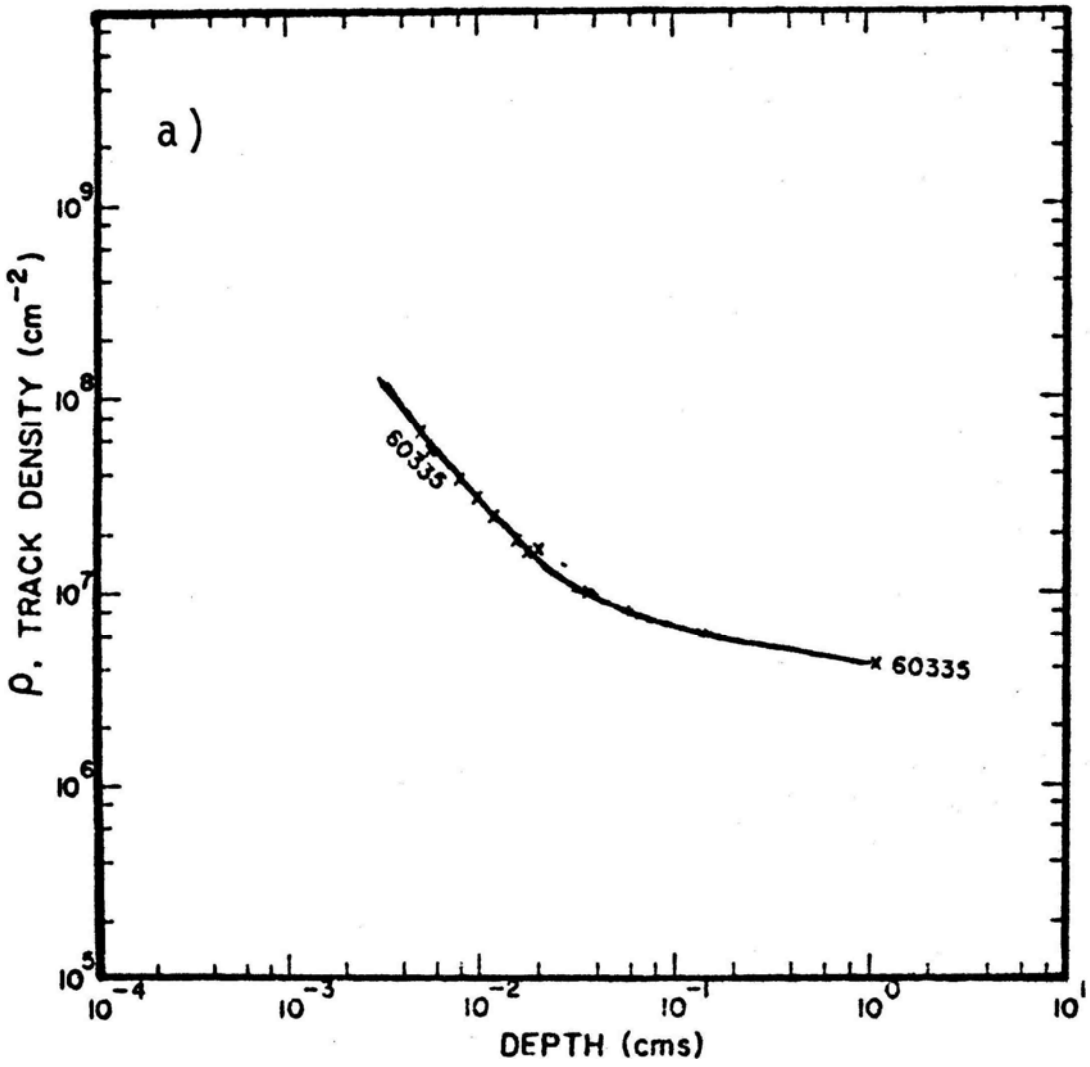

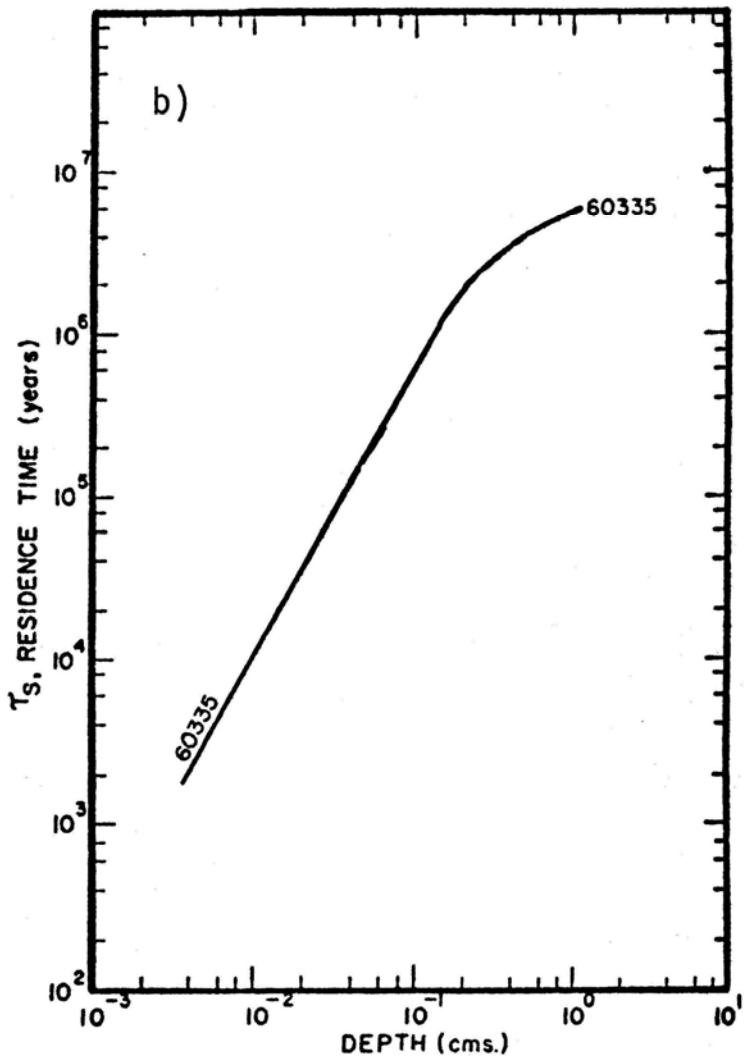

FIGURE 8. From Bhandari et al. (1976).
a) Track density profile. b) Residence time curve.

Velocity and linear strain data are provided by Warren et al. {1973) for hydrostatic and uniaxial loading conditions (Fig. 10). Bulk elastic properties calculated from the density, bulk modulus and shear modulus of the silicate phases of the rock agree well with the measured values. These authors conclude that pore and crack effects exert an extreme control over bulk elastic properties.

Simmons et al. (1975) note the presence of healed cracks that displace twin lamellae in plagioclase xenocrysts.

PROCESSING AND SUBDIVISIONS: In 1972, 60335 was cut into three main pieces, including a slab. All three of these pieces have been extensively subdivided as shown in Figure 11. Not all splits are shown. Allocations have been made from many portions of the rock.

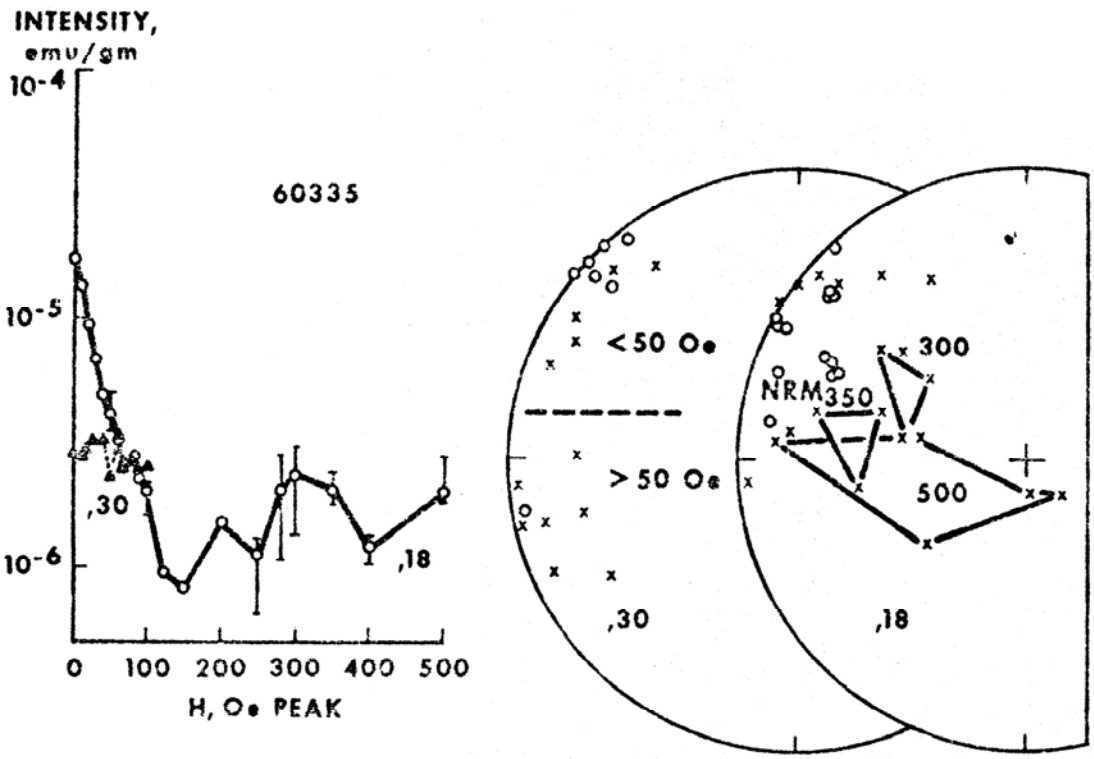

FIGURE 9. AF-demagnetization; from Pearce et el. (1973).

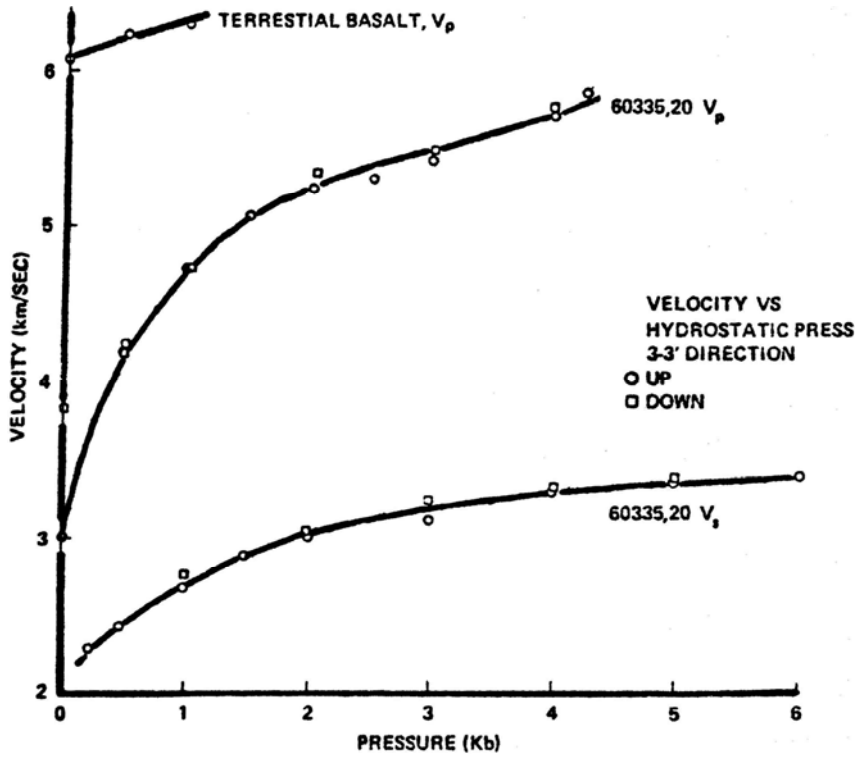

FIGURE 10. Velocity profiles; from Warren et al (1973).

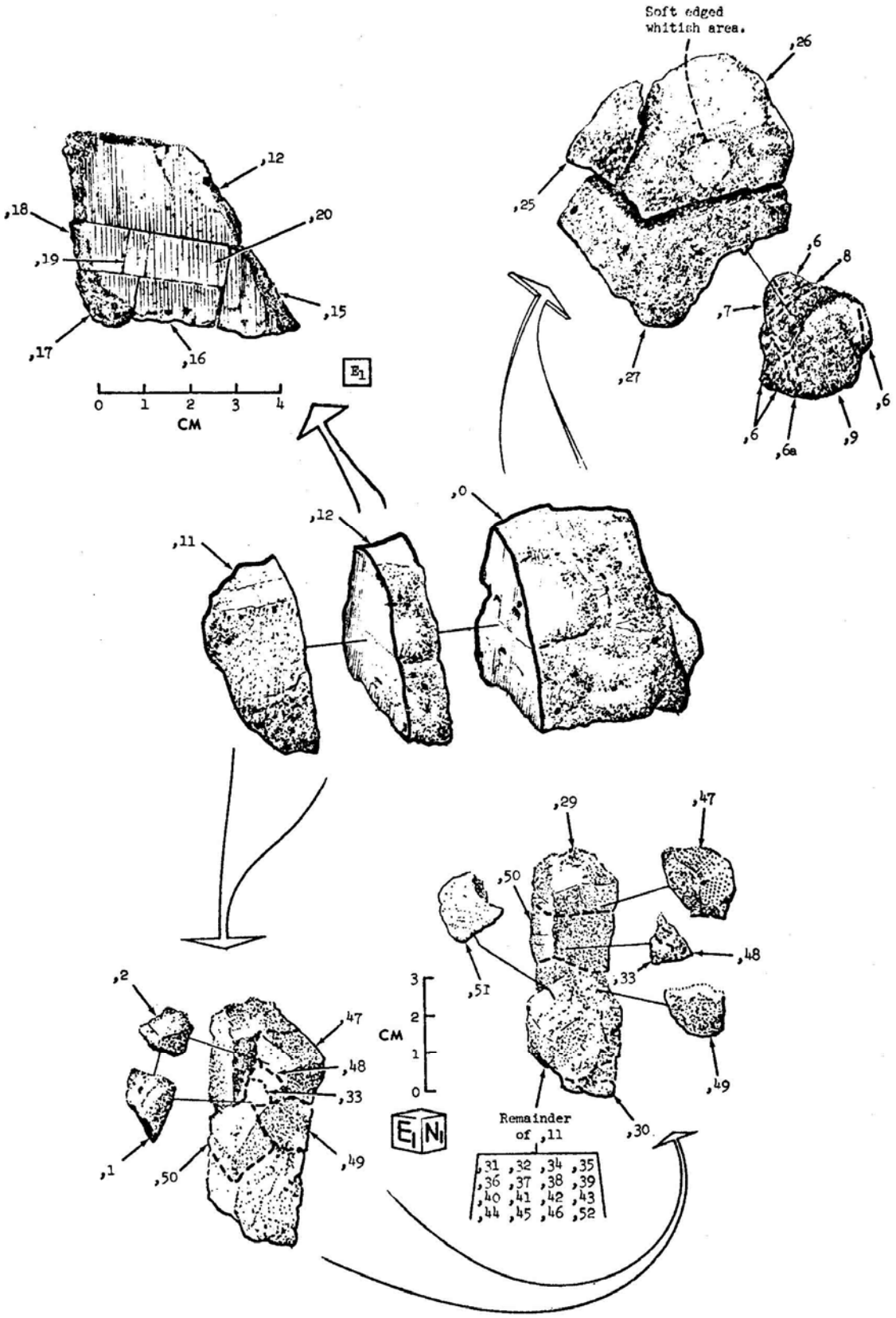

FIGURE 11. Cutting diagram.